Intermetal Oxygen Atom Transfer Reactions of Titanium Porphyrins: Complete vs Incomplete Atom Transfer. X-ray Structure of (μ-Oxo)bis[(*meso*-tetra-*p*-tolylporphyrinato)titanium(III)]

J. Alan Hays, Catherine L. Day, Victor G. Young, Jr., and L. Keith Woo,*[,1]

Department of Chemistry, Iowa State University, Ames, Iowa 50011-3111

Received July 19, 1996[⊗]

Treatment of (*meso*-tetra-*p*-tolylporphyrinato)titanium(IV) oxide, (TTP)Ti═O, with (octaethylporphyrinato)titanium-(III) chloride, (OEP)Ti−Cl, in toluene-d_8 results in the reversible exchange of axial ligands to form (TTP)Ti−Cl and (OEP)Ti═O. The net result is a formal one-electron redox process. This occurs with a second-order rate constant of $(2.4 \pm 0.2) \times 10^2$ M^{-1} s^{-1} to form an equilibrium mixture with $K = 1.7 \pm 0.4$ at 20 °C ($\Delta H^{\ddagger} = 10.8 \pm 0.4$ kcal/mol, $\Delta S^{\ddagger} = -10.7 \pm 1.2$ cal/mol·K). Use of pivalate in place of chloride on the Ti(III) complex causes no significant change in the rate of this one-electron redox process. In addition, excess chloride only partially inhibits the rate of oxygen transfer with chlorotitanium(III) complexes. A complete kinetic analysis indicates that these redox processes proceed through two parallel pathways, both involving an inner sphere μ-oxo intermediate. Competing associative and dissociative (chloride or pivalate loss) mechanisms are in effect. Reversible oxo/chloro exchange also occurs between (TTP)$TiCl_2$ and (OEP)Ti═O in $CHCl_3$ to produce (TTP)-Ti═O and (OEP)$TiCl_2$ with $K = 47 \pm 13$ and $k_f = 5 \pm 1$ M^{-1} s^{-1} at 20 °C ($\Delta H^{\ddagger} = 11 \pm 1$ kcal/mol, $\Delta S^{\ddagger} = 11 \pm 3$ cal/mol·K, $\Delta H° = -3.7 \pm 0.8$ kcal/mol, and $\Delta S° = -5 \pm 2$ cal/mol·K). In contrast, when (TTP)Ti═O is treated with (TPP)Ti(η^2-PhC≡CPh), incomplete oxygen atom transfer occurs to produce the μ-oxo complex, $[(TTP)Ti]_2O$. X-ray quality crystals of this complex can be prepared by the slow diffusion of O_2 into a solution of (TTP)Ti(4-picoline)$_2$. The structure of the μ-oxo complex, $C_{114}H_{90}N_8OTi_2$, was determined by single-crystal X-ray diffraction (crystal data: monoclinic, *C*2/*c*, $a = 32.044(8)$ Å, $b = 16.908(5)$ Å, $c = 18.525(5)$ Å, $\beta = 117.91(2)°$, $V = 8869(4)$ Å^3, $Z = 4$, $R = 5.88\%$, and $R_w = 15.38\%$). Key metrical parameters include a Ti−O distance of 1.7941(8) Å, average Ti−N distances of 2.113(3) Å, and a Ti−O−Ti angle of 170.8(2)°. The Ti atom is displaced 0.66 Å out of the mean porphyrin plane toward the oxo bridge.

Introduction

Although atom transfer reactions are very common and have been known for over 40 years, an understanding of oxygen atom transfer processes that occur between two metal complexes is still emerging.[2] A large portion of the documented oxygen atom transfer reactions take place between a metal oxo donor and non-metal oxo acceptor, such as phosphines and alkenes. Examples of intermetal oxygen-transfer reactions are less common. In most cases, reaction of a metal oxo donor with metal acceptor results in the formation of a μ-oxo species, eq 1. Holm has termed this type of reaction as incomplete atom

$$L_nM{=}O + L_nM' \rightarrow L_nM{-}O{-}M'L_n \qquad (1)$$

transfer.[3] In contrast, complete atom transfer specifies the case when the oxo ligand is totally cleaved from the donor complex, (eq 2). This case has been documented for molybdenum,[3]

$$L_nM{=}O + M'L_n \rightarrow L_nM + O{=}M'L_n \qquad (2)$$

tungsten,[3,4] and vanadium[5] complexes, and implicated in the oxoruthenium porphyrin-catalyzed aerobic epoxidation of alkenes.[6]

The fundamental factors which dictate the occurrence of complete vs incomplete oxygen atom transfer are not well understood. However, it is clear that steric factors can promote complete oxygen atom transfer by destabilizing the μ-oxo species.[7] Incomplete oxygen atom transfer typically involves a net one electron change. However, complete oxygen atom transfer can mediate both one- or two-electron redox processes. Thus an understanding of the factors that influence the electron stoichiometry involved in an oxygen atom transfer is also not well developed. Our approach toward studying these important issues has focused on systems which approach the self-exchange category ($\Delta G° = 0$). This allows an assessment of the relative stability of the incipient μ-oxo species relative to those of the oxo donor and acceptor complexes without complications arising from a thermodynamic driving force. The energetics of this bridged M−O−M unit clearly dictates the type of reaction (complete vs incomplete oxygen atom transfer) and determines the rate of atom transfer.

We have found that electronic factors are extremely important in intermetal atom transfer reactions of metalloporphyrins.[2] In the work presented here, we describe a more detailed account of oxygen atom transfer reaction between titanium porphyrin complexes.

Experimental Section

General Data. All manipulations were carried out under an atmosphere of nitrogen using either a Vacuum Atmosphere glovebox equipped with a Model MO40H Dri-Train gas purifier or on a high vacuum line using standard Schlenk techniques. All solvents were

⊗ Abstract published in *Advance ACS Abstracts,* December 1, 1996.

(1) 1990−1995 Presidential Young Investigator, 1993−1998 Dreyfus Teacher-Scholar.
(2) Woo, L. K. *Chem. Rev.* **1993**, *93*, 1125.
(3) Holm, R. H. *Chem. Rev.* **1987**, *87*, 1401.
(4) (a) Templeton, J. E.; Ward, B. C.; Chen, G. J.-J.; McDonald, J. W.; Newton, W. E. *Inorg. Chem.* **1981**, *20*, 1248. (b) Yamashita, S.; Imamura, T.; Sasaki, Y. *Chem. Lett.* **1995**, 417−418.
(5) Zhang, Y.; Holm, R. H. *Inorg. Chem.* **1990**, *29*, 911.
(6) Groves, J. T.; Quinn, R. J. *J. Am. Chem. Soc.* **1985**, *107*, 5790.
(7) Holm, R. H.; Berg, J. M. *Pure Appl. Chem.* **1984**, *56*, 1645.

S0020-1669(96)00863-4 CCC: $12.00

Table 1. Molar Absorptivities for Metalloporphyrins

	$\epsilon/(10^4\ M^{-1}\ cm^{-1})$	
	$\lambda = 572$ nm[a]	$\lambda = 550$ nm[b]
(TTP)Ti═O	0.313	2.41
(TTP)Ti−Cl	0.900	
$(TTP)TiCl_2$		1.33
(OEP)Ti═O	3.02	0.484
(OEP)Ti−Cl	1.06	
$(OEP)TiCl_2$		0.479

[a] In toluene. [b] In $CHCl_3$.

rigorously dried and degassed prior to use. Benzene-d_6, toluene, tetrahydrofuran, and hexane were vacuum distilled from purple solutions of sodium−benzophenone. Methanol was distilled from sodium under nitrogen over to 4 Å molecular sieves and then vacuum distilled a second time prior to use. CH_2Cl_2, $CDCl_3$ and CD_2Cl_2 were stored over either P_2O_5 or CaH_2 and vacuum distilled prior to use. Triphenylmethane was sublimed under reduced pressure at 100 °C prior to use. Sodium pivalate was obtained from Aldrich Chemical Co., recrystallized from methanol/CH_2Cl_2, and dried in vacuo at 125 °C. Commercially obtained (PPN)Cl was dried in vacuo at 150 °C for 24 h. (TTP)Ti═O,[8,9] (OEP)Ti═O,[8] (TTP)TiCl,[10] (OEP)TiCl,[10] and $(TTP)Ti(4\text{-picoline})_2$[11] were prepared using literature procedures. $(OEP)Ti(O_2CC(CH_3)_3)$ was prepared using a modification of a previously developed procedure.[12] All reagents used for kinetic and equilibrium studies were recrystallized twice prior to use. Concentrations of stock solutions were checked before use either by UV−vis or ^{1}H NMR spectroscopies. ^{1}H NMR spectra were recorded on either a Nicolet 300-MHz or a Varian VXR 300-MHz Fourier transform spectrometer. UV−vis data were recorded on a HP8452A diode array spectrophotometer. IR spectra were recorded on a either a IBM IR98 or a Digilab Fourier transform spectrometer.

Equilibrium Measurements. Samples for equilibrium determinations for the titanium oxo−chloride exchange and the oxo−dichloride system were prepared by adding specific volumes of known concentrations of an oxo complex, the opposing chloride or dichloride complex, and an internal standard, triphenylmethane, into a 5-mm NMR tube attached to a ground glass joint. The solvent was removed under reduced pressure in a glovebox. After adding an NMR solvent, either toluene-d_8 (oxo−chloride exchange) or $CDCl_3$ (oxo−dichloride exchange), the tube was sealed with a ground glass stopper. The tube was frozen with liquid nitrogen and flamed sealed. For the oxo−chloride system, the equilibrium constant was determined by integrating the *meso* proton signal of the (OEP)Ti═O and the pyrrole β proton signal of the (TTP)Ti═O. These signals were compared to the signal of the methine proton of the triphenylmethane to verify that mass balance was maintained and to determine concentrations. The tubes were monitored in a temperature controlled NMR probe until no further change in the spectrum was observed. For the oxo−dichloride system, all species were diamagnetic, so *meso* protons and pyrrole β protons were integrated with respect to the triphenylmethane protons to assure that mass balance was maintained.

Kinetic Measurements. Rate data for the (POR)Ti═O/(POR)Ti−X (X = chloride, pivalate anion) systems were obtained on a UV−vis spectrometer equipped with a thermally regulated cell holder. Solutions of the oxo and the appropriate titanium(III) complexes were loaded into a 1-cm quartz cuvette under nitrogen atmosphere and capped with a septum. The cuvette was placed in the cell holder, and the run was monitored at 572 nm. Molar absorptivities of the porphyrin complexes are given in Table 1. A final spectrum from 500 to 700 nm was taken to verify that decomposition of the chloride complex did not occur. Kinetic runs were also done in the presence of excess chloride in the form of bis(triphenylphosphoranylidene)ammonium chloride, (PPN)Cl. Typical initial concentrations ranged from 7.37×10^{-6} to 4.1×10^{-5} M. Rate constants were obtained using an integrated law for second order equilibrium reactions derived by King.[13]

Rate data for the (POR)Ti═O/$(POR)TiCl_2$ systems were obtained on either a UV−vis spectrophotometer with a thermally regulated cell holder (for runs at 20, 30, and 50 °C) or on a thermally regulated Varian VXR 300 MHz NMR spectrometer. For runs on the UV−vis spectrophotometer, $CHCl_3$ solutions of the oxo complex and the appropriate dichloride were loaded into a 1-cm quartz cuvette fitted with a stopcock. The cuvette was placed in the cell holder and allowed time to equilibrate to the proper temperature, and the run was monitored at 550 nm. Molar absorptivities of the porphyrin complexes in $CHCl_3$ are given in Table 1. A final spectrum from 500 to 700 nm was obtained to verify that the dichloride complexes had not decomposed. Typical concentrations of oxo and dichloride complexes were approximately 4.5×10^{-5} M. For kinetic runs at 0 °C, solutions of the oxo complex, the appropriate dichloride complex, and a internal standard, triphenylmethane, were transferred into a 5-mm NMR tube fitted with a ground glass joint. The solvents were removed under reduced pressure and a high vacuum line adapter was attached. Deuterated solvent was vacuum transferred into the tube on a high vacuum line, the tube was backfilled with N_2 to approximately 550 mm Hg, and the NMR tube was flame sealed. The tube was kept in liquid N_2 prior to insertion into the instrument, and then it was thawed slightly and placed into the magnet and allowed to equilibrate to the proper temperature. Runs were monitored with either the meso protons of the OEP complexes or the pyrrole β protons of the TPP complexes and integrated with respect to the methine proton of the internal standard. Comparison of these signals is used to verify that mass balance was maintained during the run. In both cases, rate constants were obtained using an integrated rate law for second-order equilibrium reactions derived by King.[13]

Synthesis of $[(TPP)Ti]_2O$. A solution of (TTP)Ti═O (18 mg, 24 μmol) and $(TTP)Ti(\eta^2\text{-PhC}{\equiv}\text{CPh})$ (22 mg, 25 μmol) in 10 mL of toluene was stirred under N_2. Over 3 h, the bright ruby red solution turned brick red with formation of a precipitate. After the mixture was cooled at −20 °C for 16 h, a brick red product (15.6 mg, 48%) was isolated by filtering and washing with neat toluene and neat hexane and was dried in vacuo at 100 °C for 5 h. ^{1}H NMR ($CDCl_3$): δ 2.68 (br, s, CH_3). UV−vis (toluene): 424 (Soret), 550 nm.

X-ray Structure Determination of $[(TTP)Ti]_2O$. Crystals of $[(TTP)Ti]_2O$ were grown from slowly diffusing O_2 into a solution of $(TTP)Ti(4\text{-picoline})_2$ in benzene/octane at ambient temperature. A brown prismatic crystal ($0.35 \times 0.35 \times 0.15$ mm) was attached to the tip of a glass fiber and mounted on a Siemens P4/RA diffractometer for data collection at -80 ± 1 °C using Cu Kα radiation ($\lambda = 1.541\ 78$ Å). Cell constants were determined from a list of reflections found by a rotation photograph. Lorentz and polarization corrections were applied. A correction based on a nonlinear decay in the standard reflections of 5.8% was applied to the data. An absorption correction based on a series of azimuthal scans using the semiempirical method was applied. The agreement factor for the averaging of observed reflections was 2.1% (based on *F*).

The centric space group *C*2/*c*, was indicated by systematic absences and intensity statistics.[14] The positions of all non-hydrogen atoms were determined by Fourier techniques. All non-hydrogen atoms were refined with anisotropic thermal parameters. After the least-squares refinement converged, all hydrogen atoms were placed at calculated positions 0.95 Å from the attached carbon with isotropic temperature factors set at a default value of 0.08 Å^2. The hydrogens on the porphyrin ring were later refined isotropically. The asymmetric unit contains 1.5 benzene molecules. The hydrogens of the benzene molecules were refined with isotropic temperature factors.

(8) Fournari, C.; Guilard, R.; Fontesse, M.; Latour, J.-M.; Marchon, J.-C. *J. Organomet. Chem.* **1976**, *110*, 205.
(9) Abbreviations: TTP is the dianion of *meso*-tetra-*p*-tolylporphyrin, TPP is the dianion of *meso*-tetraphenylporphyrin, and OEP is the dianion of octaethylporphyrin.
(10) Berreau, L. M.; Hays, J. A.; Young, V. G., Jr.; Woo, L. K. *Inorg. Chem.* **1994**, *33*, 105.
(11) Hays, J. A.; Young, V. G., Jr.; Day, C. L.; Caron, C.; D'Souza, F.; Kadish, K. M.; Woo, L. K. *Inorg. Chem.* **1993**, *32*, 4186.
(12) Woo, L. K.; Goll, J. G.; Czapla, D. J.; Hays, J. A. *J. Am. Chem. Soc.* **1991**, *113*, 8478.
(13) King, E. L. *Int. J. Chem. Kinet.* **1982**, *14*, 1285. For a second-order reversible reaction, A + B ⇌ C + D, Δ is the displacement of any species from its equilibrium value. $\Delta = [A] - [A]_\infty = [B] - [B]_\infty = [C]_\infty - [C] = [D]_\infty - [D]$ and $\alpha = [A]_\infty + [B]_\infty + ([C]_\infty + [D]_\infty)/K$.
(14) SHELXTL PLUS. Siemens Industrial Automation, Inc., Madison, WI.

Table 2. Rate Constants for Oxo Transfer

T/(°C)	K_3[a]	$k_3/10^2$ M^{-1} s^{-1} [a]	K_6[b]	k_6/M^{-1} s^{-1} [b]
50			26 ± 10	58 ± 7
40		8.1 ± 1.1		
30	1.4 ± 0.4	4.6 ± 0.2	31 ± 8	7 ± 2
20	1.7 ± 0.4	2.4 ± 0.2	47 ± 13	5 ± 1
10	1.4 ± 0.4	1.4 ± 0.3		
0	1.3 ± 0.3	0.56 ± 0.09	71 ± 11	0.18 ± 0.08

[a] In toluene. [b] In $CHCl_3$.

The X-ray data collection was carried out at the Iowa State University Molecular Structure Laboratory. Refinement calculations were performed on a SGI INDY R4400-SC or a Pentium computer using the SHELXTL version 5.0 programs.

Results

Reduction of Oxotitanium(IV) Porphyrin with Titanium(III) Porphyrin. Treatment of (TTP)Ti═O with (OEP)Ti—Cl in toluene-d_8 results in spectral changes which are consistent with the transfer of a terminally bound oxygen ligand between two metal complexes shown in eq 3. The ^{1}H NMR spectrum

$$\text{(TTP)Ti═O} + \text{(OEP)Ti—Cl} \underset{k_{-3}}{\overset{k_3}{\rightleftharpoons}} \text{(TTP)Ti—Cl} + \text{(OEP)Ti═O} \quad (3)$$

of the resulting mixture contains a new resonance at 10.54 ppm indicating the formation of (OEP)Ti═O. The resonance for (TTP)Ti═O at 9.24 ppm does not completely disappear indicating that eq 3 is an equilibrium process. Since the titanium(III) complexes are d^1 and paramagnetic, the signals for these species are extremely broadened and often not observed. The reversibility of eq 3 can be confirmed by the complementary experiment in which (OEP)Ti═O is treated with (TTP)Ti—Cl. This generates a final spectrum with peak positions identical to that observed for the forward process.

Equilibrium constants for eq 3 were established by using ^{1}H NMR to monitor the pyrrole β proton resonance of (TTP)Ti═O (9.24 ppm), the *meso* proton signal of (OEP)Ti═O (10.54 ppm), and the methine proton of the internal standard, triphenylmethane (5.34 ppm). Flamed-sealed NMR tubes containing (TTP)Ti═O, (OEP)Ti—Cl, and triphenylmethane in toluene-d_8 were prepared. During the course of the experiment, mass balance was maintained in terms of total oxo complex concentration. The equilibrium constants for eq 3, determined over a 40-deg range, were all very close to $K_3 = 1.5 \pm 0.4$ and are listed in Table 2. Small errors in integration of proton resonances lead to a relatively wide range of standard deviations in calculated equilibrium constants. Thus, a reliable temperature dependence could not be obtained.

The forward rates of eq 3 in toluene were determined spectrophotometrically by following the absorbance changes at 572 nm. A summary of rate constants is listed in Table 2. All of the compounds involved, (TTP)Ti═O, (TTP)Ti—Cl, (OEPTi═O, and (OEP)Ti—Cl, obey Beer's law over the concentration range used in these experiments. This indicates self-association does not complicate the mechanistic analysis. In all kinetic runs, the data were found to obey an integrated rate law for reversible second-order reactions shown in eq 4.[13] Plots

$$\ln\left[\frac{\Delta}{\alpha + \Delta(1 + 1/K)}\right] = -\alpha k t + \text{constant} \quad (4)$$

of $\ln[\Delta/(\alpha + \Delta(1 - 1/K))]$ vs time are linear for at least 3 half-lives. An absorbance vs time curve of a typical kinetic run and a log plot of the data are shown in Figure 1.

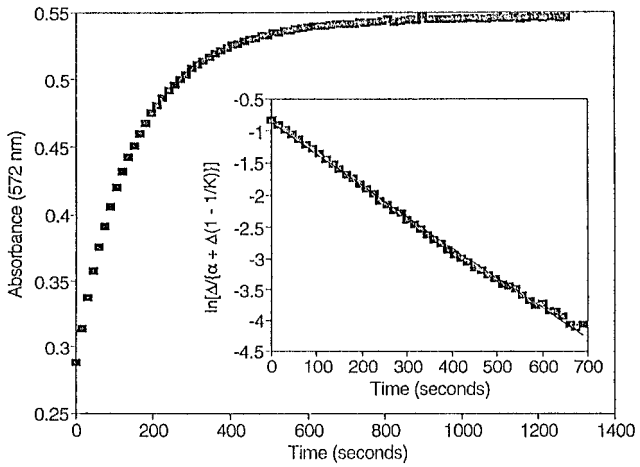

Figure 1. Representative absorption vs time plot for reaction 3. $[(TTP)Ti═O]_o = 1.95 \times 10^{-5}$ M and $[(OEP)TiCl]_o = 1.94 \times 10^{-5}$ M, in toluene at 20 °C. Inset shows plot of $\ln[\Delta/(\alpha + \Delta(1 + 1/K))]$ vs t, $k_f = 240 \pm 20$ M^{-1} s^{-1}.

Effect of Solvent. (POR)Ti—X complexes (X is an anionic ligand) are known to coordinate neutral donor ligands on the back side of the metal,[15,16] so the forward rates of eq 3 in THF were examined. In all runs the data were found to follow second-order reversible rate law for more than 3 half-lives. Rates at 20 °C for eq 3 were found to exhibit a moderate dependence on solvent used ($k_{THF} = 70$ M^{-1} s^{-1}, $k_{toluene} = 240$ M^{-1} s^{-1}, and $k_{CH_2Cl_2} = 460$ M^{-1} s^{-1}). A similar solvent effect was observed for the system where chromium was used instead of titanium.[17]

Effect of Axial Ligand. Axial ligand effects were studied in these systems by changing the monoanionic ligand of the starting titanium(III) porphyrin complexes as shown in eq 5. A

$$\text{(TTP)Ti═O} + \text{(OEP)Ti—X} \underset{k_{-5}}{\overset{k_5}{\rightleftharpoons}} \text{(TTP)Ti—X} + \text{(OEP)Ti═O} \quad (5)$$

comparison of two different axial ligands, pivalate and chloride, was made at 20 °C in THF. Kinetic runs for the pivalate system were found to follow an integrated rate law for second-order reversible reactions. Rates for eq 5 were found to have little dependence on the nature of the axial ligand (at 20 °C: $k_{piv} = 100 \pm 10$ M^{-1} s^{-1} and $k_{chloride} = 70 \pm 10$ M^{-1} s^{-1}).

Effect of Added Axial Ligand. The rate of oxygen atom transfer was studied as a function of added chloride ion. Bis(triphenylphosphoranylidene)ammonium chloride, (PPN)Cl, was used as the source of chloride. Due to the low solubility of (PPN)Cl in toluene, kinetic runs were performed in CH_2Cl_2 solutions. The dissociation constant for (PPN)Cl at 20 °C in CH_2Cl_2 is 5.10×10^{-4}.[18]

The rate data for all runs in CH_2Cl_2 were found to follow a second-order reversible rate law at 20 °C. In the absence of any added chloride, the rate constant for the eq 3 in CH_2Cl_2 at 20 °C is $(4.6 \pm 0.4) \times 10^2$ M^{-1} s^{-1}. A 23-fold excess of Cl$^-$, with respect to (OEP)TiCl, decreases the rate constant to $(4.3 \pm 0.3) \times 10^2$ M^{-1} s^{-1}; a 54-fold excess of [Cl$^-$] resulted in a rate constant of $(3.9 \pm 0.3) \times 10^2$ M^{-1} s^{-1}. Using a 427-fold excess, the rate constant was only reduced to $(2.6 \pm 0.3) \times 10^2$ M^{-1} s^{-1}.

(15) Latour, J.-M.; Marchon, J.-C.; Nakajima, M. *J. Am. Chem. Soc.* **1979**, *101*, 3974.
(16) Marchon, J.-C.; Latour, J.-M.; Boreham, C. J. *J. Mol. Catal.* **1980**, *7*, 227.
(17) Woo, L. K.; Goll, J. G.; Berreau, L. B.; Weaving, R. *J. Am. Chem. Soc.* **1992**, *114*, 7411.
(18) Algra, G. P.; Balt, S. *Inorg. Chem.* **1981**, *20*, 1102.

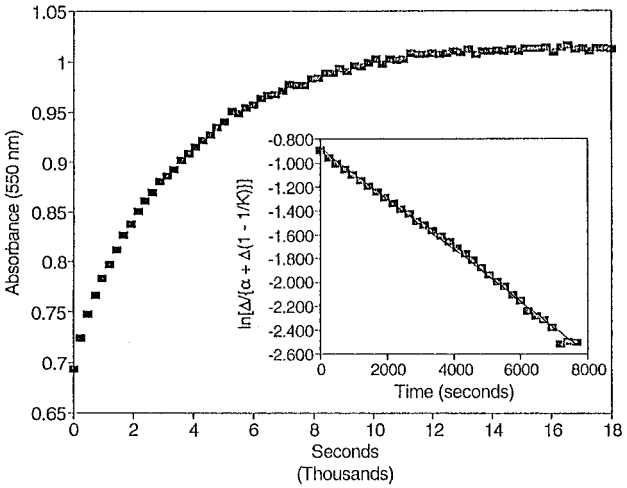

Figure 2. Absorption vs time plot of reaction 6. $[(TTP)TiCl_2]_o = 4.44 \times 10^{-5}$ M and $[(OEP)Ti{=}O]_o = 4.41 \times 10^{-5}$ M, in $CHCl_3$ at 20 °C. Inset shows plot of $\ln[\Delta/(\alpha + \Delta(1 + 1/K))]$ vs t, $k_f = 5 \pm 1$ M^{-1} s^{-1}.

Oxygen Atom Transfer between (TTP)TiCl$_2$ and (OEP)Ti=O. Treatment of $(TTP)TiCl_2$ with (OEP)Ti=O in $CDCl_3$ results in spectral changes consistent with the transfer of a terminally bound oxo ligand between two metal centers (eq 6).

$$(TTP)TiCl_2 + (OEP)Ti{=}O \underset{k_{-6}}{\overset{k_6}{\rightleftharpoons}} (TTP)Ti{=}O + (OEP)TiCl_2 \quad (6)$$

All species are diamagnetic making it easy to verify that transfer has occurred. The ^{1}H NMR spectrum of the resulting mixture contains two new signals at 10.48 and 9.12 ppm indicating the formation of $(OEP)TiCl_2$ and (TTP)Ti=O, respectively. The signals for (TTP)Ti=O (8.99 ppm) and (OEP)Ti=O (10.54 ppm) do not entirely disappear indicating that eq 6 is an equilibrium process. The equilibrium (eq 6) can be verified by the reverse process in which (TTP)Ti=O is treated with $(OEP)TiCl_2$. This generates a final spectrum identical to that observed for the forward process.

Equilibrium constants for eq 6 are once again conveniently established by ^{1}H by monitoring all *meso* proton and pyrrole β proton signals, since all species are diamagnetic. Flamed-sealed NMR tubes were prepared containing $(TTP)TiCl_2$ and (OEP)Ti=O plus an internal standard, triphenylmethane in $CDCl_3$. Initial concentrations for the porphyrin complexes range from 0.5 to 2.0 mM. During the course of the experiment, mass balance was maintained. The equilibrium constants to eq 6 were determined over a 50-deg range and are listed in Table 2. The thermodynamic parameters, $\Delta H_6^\circ = -3.7 \pm 0.8$ kcal/mol and $\Delta S_6^\circ = -5.1 \pm 0.7$ cal(mol·K)$^{-1}$, were determined from this temperature dependence.

The forward rates of eq 6 in $CHCl_3$ (Table 2) were examined both by spectrophotometric methods, monitoring the absorbance changes at 550 nm, and by ^{1}H NMR, observing the spectral changes of the *meso* and pyrrole β protons. For the UV−vis runs, all compounds listed in Table 1 obey Beer's law over the concentration range of the experiments. This indicates self-association does not complicate the mechanistic analysis. In all kinetic runs, the data are found to obey an integrated rate law for reversible second-order reactions as shown in eq 4. Plots of $\ln[\Delta/(\alpha + \Delta(1 - 1/K))]$ vs time are linear for at least 3 half lives. A typical kinetic curve and the corresponding log plot are illustrated in Figure 2.

Reduction of (TTP)Ti=O with (TTP)Ti(η^2-PhC≡CPh). When (TTP)Ti=O is treated anaerobically with the Ti(II) complex, (TTP)Ti(η^2-PhC≡CPh), in a sealed NMR tube, loss of all of the ^{1}H NMR signals for the starting materials is observed. The final NMR spectrum contains peaks due to free diphenyl acetylene and a broad resonance at 2.68 ppm from a new paramagnetic μ-oxo product, $[(TTP)Ti]_2O$ (eq 7). The Ti−O−Ti dimer can be cleanly converted to (TTP)Ti=O on treatment with O_2. Despite repeated attempts, it has not been possible to prepare pure samples of $[(TTP)Ti]_2O$ which are free of the terminal oxo complex, (TTP)Ti=O. Nonetheless, X-ray quality single crystals of $[(TTP)Ti]_2O$ were produced by slow diffusion of O_2 into a benzene/octane solution of the Ti(II) complex, (TTP)Ti(4-picoline)$_2$.

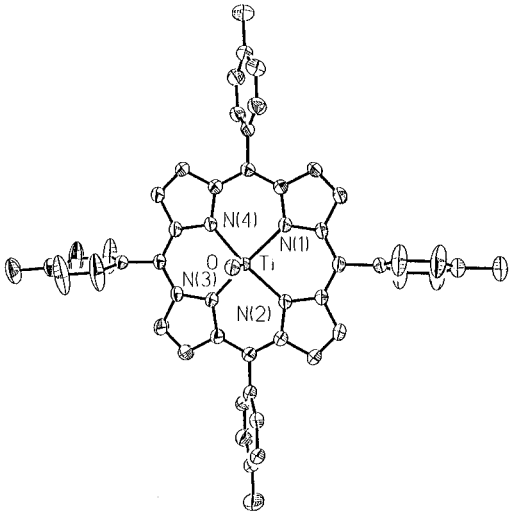

Figure 3. Molecular structure for the asymmetric unit of $[(TTP)Ti]_2O$. Thermal ellipsoids are drawn at the 30% probability level.

$$(TTP)Ti{=}O + (TTP)Ti(PhC{\equiv}CPh) \rightleftarrows [(TTP)Ti]_2O + PhC{\equiv}CPh \quad (7)$$

X-ray Structure of [(TPP)Ti]$_2$O. The molecular structure of $[(TTP)Ti]_2O$ was determined by single-crystal X-ray diffraction. Thermal ellipsoids and the atom numbering scheme of the asymmetric unit are shown in Figure 3. Crystallographic data for the structure determination are listed in Table 3 and fractional coordinates for the non-hydrogen atoms are in Table 4. Selected bond distances and angles are given in Table 5.

The structure determination of $[(TTP)Ti]_2O$ confirms its formulation as a neutral μ-oxo-bridged Ti(III) dimer. The Ti atom resides in a square pyramidal coordination sphere formed by four basal pyrrole nitrogens and an apical oxygen atom with the Ti displaced from the N_4 plane 0.66 Å toward the bridging oxygen. The average metrical parameters for the porphyrin skeleton are $N-C_\alpha = 1.397(5)$ Å, $C_\alpha-C_\beta = 1.436(6)$ Å, $C_{\beta1}-C_{\beta2} = 1.347(6)$ Å, $C_\alpha-C_{meso} = 1.401(6)$ Å, and $C_{meso}-C_{ipso} = 1.494(6)$ Å. These bond lengths are comparable to those found in other porphyrin complexes.[19] In addition, the porphyrin ligand has an S_4-type ruffling in which the meso carbons are alternately displaced 0.08 Å above and below the mean porphyrin plane. The Ti−O distance of 1.794 (1) Å is shorter than that expected for a Ti−O single bond (ca. 2.0 Å)[20] but is very similar to the Ti−O distance (1.77(1) Å) found in $(TPP)Ti-OCH_3$[21] and falls in the range observed for other Ti−O−Ti fragments.[22] The two mean porphyrin planes in

(19) (a) Scheidt, W. R. In *The Porphyrins*, Dolphin, D., Ed.; Academic Press: New York, 1978; Vol. III, Chapter 10. (b) Scheidt, W. R.; Lee, Y. J. *Struct. Bonding* **1987**, *64*, 1.
(20) Peterson, J. L. *Inorg. Chem.* **1981**, *20*, 181.
(21) Boreham, C. J.; Buisso, G.; Duee, E.; Jordanov, J.; Latour, J.-C.; Marchon, J.-C. *Inorg. Chim. Acta* **1983**, *70*, 77.

Table 3. Crystallographic Parameters for $[(TTP)Ti]_2O\cdot 3C_6H_6$

empirical formula: $C_{114}H_{90}N_8O_1Ti_2$
fw = 1683.78
cryst syst: monoclinic
space group *C*2/*c*
unit cell dimens
$a = 32.044(8)$ Å
$b = 16.908(5)$ Å
$c = 18.525(5)$ Å
$\beta = 117.91(2)°$
$V = 8869(4)$ Å^3
Z = 4
d(calcd) = 1.261 g/cm^3
abs coeff: 1.975 mm^{-1}
$F(000) = 3528$
radiation: Cu Kα ($\lambda = 1.54178$ Å)
$T = 193(2)$ K
θ range: 3.04−57.15°
monochromator: highly oriented graphite cryst
no. of reflcns collcd: 11 953
no. of independent reflcns: 5983 ($R_{int} = 4.07\%$)
no. of observed reflcns: 4570 ($F > 6.0\sigma(F)$)
max and min transm: 1.000 and 0.6090
no. of params refined: 568
final *R* indices (obs data): $R = 5.88\%$, $R_w = 15.38\%$
goodness-of-fit on F^2: 1.060
data-to-param ratio: 8.0:1
largest difference peak: +0.458 e Å^{-3}
largest difference hole: −0.444 e Å^{-3}

$[(TTP)Ti]_2O$ deviate from a parallel arrangement by only 5.7°. In addition, the two porphyrin ligands are staggered 26.4° about the Ti_a-Ti_b axis from the eclipsed geometry. The Ti−O−Ti alignment is nearly linear with a bond angle of 170.9(2)°. Thus, $[(TTP)Ti]_2O$ is essentially isostructural with $[(TPP)Fe]_2O$,[23] but notably different from the scandium analog, $[(TTP)Sc]_2O$, where Sc−O−Sc angles are 109(3) and 111(3)°.[24]

Discussion

We have found that complete oxygen atom transfer resulting in either one- or zero-electron exchange between two metalloporphyrins can be achieved. It is possible to observe this process by using different porphyrin ligands as UV−vis and ^{1}H NMR spectroscopic labels. An additional benefit derived from the use of metalloporphyrins arises from the structural integrity maintained by these complexes throughout the reaction, eliminating complications due to ligand loss. Furthermore, stereochemical rearrangements found in other systems that undergo complete atom transfer are not possible here.[3,25] Rate constants for eq 3 have been measured in the forward direction over a 40-deg temperature span in toluene. These rate constants range between 60 and 810 M^{-1} s^{-1}. The temperature dependence of the forward rate yields activation parameters of $\Delta H^{\ddagger}_3 = 10.8 \pm 0.4$ kcal/mol and $\Delta S^{\ddagger}_3 = -10.7 \pm 1.2$ cal(mol·K)$^{-1}$. Rate constants for eq 6 have been measured in the forward direction over a 50-deg temperature range in CH_2Cl_2. These rate constants range between 0.18 and 58 M^{-1} s^{-1}. The temperature dependence of the forward rate constants yield activation parameters of $\Delta H^{\ddagger}_6 = 11 \pm 1$ kcal/mol and $\Delta S^{\ddagger}_6 = 11 \pm 3$ cal(mol·K)$^{-1}$. Although eq 3 proceeds, in all probability, by an inner sphere process, mechanistic aspects of this reaction are complicated by the bridging abilities of both the chloride and oxo ligands. In order to address this issue, we have compared the reduction of (TTP)Ti═O with that of both (OEP)Ti−Cl and $(OEP)Ti-O_2CC(CH_3)_3$. The rate constants for these two reaction are similar, regardless of whether chloride ($k_{Cl} = 70$ M^{-1} s^{-1}) or pivalate ($k_{piv} = 100$ M^{-1} s^{-1}) is the axial ligand on titanium(III). Because pivalate is a much bulkier ligand, this rate comparison serves to rule out a binuclear intermediate in which the monoanionic ligand is involved in bridging the

Table 4. Atomic Coordinates ($\times 10^4$) and Equivalent Isotropic Displacement Coefficients (Å^2 $\times$ 10^3) for $[(TTP)Ti]_2O\cdot 3C_6H_6$

	x	*y*	*z*	*U*(eq)	SOF
Ti	4945(1)	1537(1)	6494(1)	29(1)	1
O	5000	1451(2)	7500	41(1)	1
N(1)	4324(1)	2196(2)	5811(2)	33(1)	1
N(2)	5310(1)	2570(2)	6464(2)	33(1)	1
N(3)	5523(1)	929(2)	6492(2)	36(1)	1
N(4)	4543(1)	543(2)	5851(2)	33(1)	1
C(1)	3869(1)	1913(2)	5431(2)	37(1)	1
C(2)	3546(1)	2564(2)	5169(2)	46(1)	1
C(3)	3800(1)	3232(2)	5392(2)	44(1)	1
C(4)	4288(1)	3011(2)	5793(2)	36(1)	1
C(5)	4664(1)	3547(2)	6073(2)	35(1)	1
C(51)	4553(1)	4415(2)	5984(2)	37(1)	1
C(52)	4592(2)	4851(3)	5396(3)	82(2)	1
C(53)	4491(2)	5652(3)	5298(3)	88(2)	1
C(54)	4355(1)	6045(2)	5781(3)	53(1)	1
C(55)	4332(2)	5620(3)	6370(4)	87(2)	1
C(56)	4430(2)	4814(3)	6475(3)	76(2)	1
C(57)	4244(2)	6919(3)	5649(4)	77(2)	1
C(6)	5140(1)	3335(2)	6388(2)	34(1)	1
C(7)	5522(1)	3883(2)	6633(2)	39(1)	1
C(8)	5920(1)	3461(2)	6837(2)	40(1)	1
C(9)	5789(1)	2639(2)	6732(2)	35(1)	1
C(10)	6101(1)	2016(2)	6851(2)	38(1)	1
C(101)	6605(1)	2210(2)	7118(2)	40(1)	1
C(102)	6889(1)	2559(2)	7878(2)	42(1)	1
C(103)	7355(1)	2743(2)	8112(3)	46(1)	1
C(104)	7557(1)	2586(2)	7612(3)	51(1)	1
C(105)	7276(1)	2226(3)	6864(3)	56(1)	1
C(106)	6809(1)	2045(2)	6618(3)	50(1)	1
C(107)	8063(2)	2805(3)	7854(3)	70(1)	1
C(11)	5972(1)	1216(2)	6734(2)	40(1)	1
C(12)	6290(1)	575(2)	6880(3)	55(1)	1
C(13)	6040(1)	−104(2)	6729(3)	55(1)	1
C(14)	5560(1)	115(2)	6483(2)	38(1)	1
C(15)	5189(1)	−423(2)	6266(2)	36(1)	1
C(151)	5318(1)	−1281(2)	6370(2)	36(1)	1
C(152)	5292(3)	−1733(3)	5753(3)	92(2)	1
C(153)	5439(2)	−2508(3)	5862(3)	90(2)	1
C(154)	5616(1)	−2862(2)	6585(3)	50(1)	1
C(155)	5652(3)	−2406(3)	7213(3)	118(3)	1
C(156)	5502(3)	−1624(3)	7103(3)	103(2)	1
C(157)	5782(2)	−3713(3)	6706(3)	79(2)	1
C(16)	4716(1)	−218(2)	5961(2)	35(1)	1
C(17)	4333(1)	−773(2)	5700(2)	46(1)	1
C(18)	3932(1)	−347(2)	5431(2)	47(1)	1
C(19)	4060(1)	476(2)	5516(2)	38(1)	1
C(20)	3742(1)	1106(2)	5301(2)	37(1)	1
C(201)	3228(1)	903(2)	4879(2)	39(1)	1
C(202)	2933(1)	1088(2)	5216(2)	49(1)	1
C(203)	2461(1)	868(3)	4822(3)	54(1)	1
C(204)	2271(1)	457(2)	4096(3)	51(1)	1
C(205)	2564(1)	277(2)	3765(3)	51(1)	1
C(206)	3034(1)	501(2)	4145(2)	45(1)	1
C(207)	1757(1)	218(3)	3684(3)	74(2)	1
C(301)	2557(2)	128(3)	1558(3)	75(1)	1
C(302)	2274(2)	776(3)	1337(3)	77(1)	1
C(303)	1824(2)	721(3)	1232(4)	92(2)	1
C(304)	1653(2)	16(3)	1342(4)	95(2)	1
C(305)	1937(2)	−640(3)	1557(3)	75(1)	1
C(306)	2389(2)	−587(3)	1674(3)	72(1)	1
C(307)	2579(6)	8300(7)	4983(8)	164(5)	1
C(308)	2130(5)	7981(8)	4563(8)	171(5)	1
C(309)	2064(4)	7200(7)	4595(6)	173(4)	1

(22) Orpen, A. G.; Brammer, L.; Allen, F. H.; Kennard, O.; Watson, D. G.; Taylor, R. *J. Chem. Soc., Dalton Trans.* **1989**, S1.
(23) Hoffman, A. B.; Collins, D. M.; Day, V. W.; Fleischer, E. B.; Srivastava, T. S.; Hoard, J. L. *J. Am. Chem. Soc.* **1972**, *94*, 3620.
(24) Sewchok, M. G.; Haushalter, R. C.; Merola, J. S. *Inorg. Chim. Acta* **1988**, *144*, 47.
(25) Holm, R. H. *Coord. Chem. Rev.* **1990**, *100*, 183.

Table 5. Selected Bond Lengths (Å) and Angles (deg) for $[(TTP)Ti]_2O\cdot 3C_6H_6$

Ti−O	1.7941 (8)	Ti−N(3)	2.118 (3)
Ti−N(1)	2.110 (3)	Ti−N(4)	2.114 (3)
Ti−N(2)	2.119 (3)	N(1)−C(1)	1.376 (5)
O−Ti−N(1)	105.7(1)	O−Ti−N(4)	105.0(1)
O−Ti−N(2)	107.8(1)	N(1)−Ti−N(4)	85.8(1)
N(1)−Ti−N(2)	85.8(1)	N(2)−Ti−N(4)	147.1(1)
O−Ti−N(3)	107.5(1)	N(3)−Ti−N(4)	85.2(1)
N(1)−Ti−N(3)	146.7(1)	Ti−O−Ti #1	170.8(2)
N(2)−Ti−N(3)	84.6(1)		

Scheme 1

$$\text{Ti-Cl} \rightleftharpoons \text{Ti(III)}^+ + \text{Cl}^- \qquad K$$

$$\text{Ti(III)}^+ + \text{Ti=O} \rightarrow \text{products} \qquad k_{S_N1}$$

$$\text{Ti-Cl} + \text{Ti=O} \rightarrow \text{products} \qquad k_{S_N2}$$

$$\text{Ti} = \text{(Por)Ti}$$

two metals. Thus the μ-chloro-bridged adduct, **A**, and the doubly bridged species, **B**, must not be important intermediates along the reaction pathway.

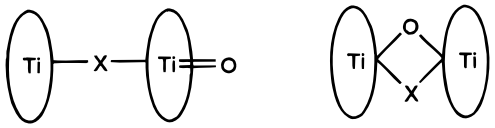

A **B**

It is likely that the redox reaction between (TTP)Ti=O and (OEP)Ti−Cl involves a μ-oxo intermediate. The single-crystal X-ray structure of (TTP)Ti−O−Ti(TTP) serves as a model for this bridged intermediate. Formation of the μ-oxo intermediate can occur either by an S_N1-type or an S_N2-type mechanism. These two processes differ primarily by the timing in which Cl^- dissociates—prior to or subsequent to formation of the binuclear μ-oxo species. Note that added Cl^- weakly inhibits the oxo transfer in eq 3. Formation of a six-coordinate anion, $[(OEP)TiCl_2]^-$, which slows the formation of a μ-oxo intermediate is unlikely since related porphyrin complexes show little affinity for an anionic ligand.[26] The important steps to consider in unravelling the mechanism are shown in Scheme 1. The integrated rate law derived from Scheme 1 is given in eq 8.

$$\frac{d[\text{products}]}{dt} = \left\{\frac{k_{S_N1}K + k_{S_N2}[Cl^-]}{K + [Cl^-]}\right\}[\text{Ti—Cl}][\text{Ti=O}] \qquad (8)$$

The apparent rate constant, k_{app}, and observed chloride ion dependencies in CH_2Cl_2 were found to fit eq 8 with values of $k_{S_N1} = (4.8 \pm 0.3) \times 10^2$ and $k_{S_N2} = (2.3 \pm 0.9) \times 10^2$ M^{-1} s^{-1}. Thus both S_N1- and S_N2-type pathways occur as competing processes. This is consistent with the weak chloride inhibition results. In addition, the small rate reduction in a coordinating solvent such as THF is presumably due to inhibition of both S_N1 and S_N2 pathways.

The reduction products of oxotitanium porphyrins are strongly dependent on the nature of the reducing agent. This behavior is analogous to the inner sphere reduction of oxochromium(IV) porphyrin complexes. When chromium(II) porphyrin is the reducing agent, the reaction halts at the μ-oxo dimer.[27] However, when a chromium(III) porphyrin is used as the reductant, the result is reversible oxygen atom transfer. In the case of oxotitanium(IV) porphyrins, we observe similar results. Mechanistic evidence for the Ti=O/Ti−X reaction (eq 3) is consistent with a pathway which involves a μ-oxo intermediate, $[Ti^{IV}—O—Ti^{III}]^{5+}$. Single-electron transfer within this activated complex always produces one metal in a +IV oxidation state. The instability of $[Ti^{IV}—O—Ti^{III}]^{4+}$ relative to the structurally characterized $[Ti^{III}—O—Ti^{III}]^{4+}$ complex may simply reflect an inherent tendency for the Ti(IV) d^0 center and the oxo ligand to form a strong metal−oxygen double bond rather than for the oxo ligand to form two M−O single bonds. Thus, a key difference between the stability of the two μ-oxo species, $[Ti^{IV}—O—Ti^{III}]^{5+}$ and $[Ti^{III}—O—Ti^{III}]^{4+}$, solely may be a matter of oxidation state and the d-electron configuration. In order to form $O=Ti^{IV}$, the III−III complex must disproportionate while the III−IV intermediate simply dissociates.

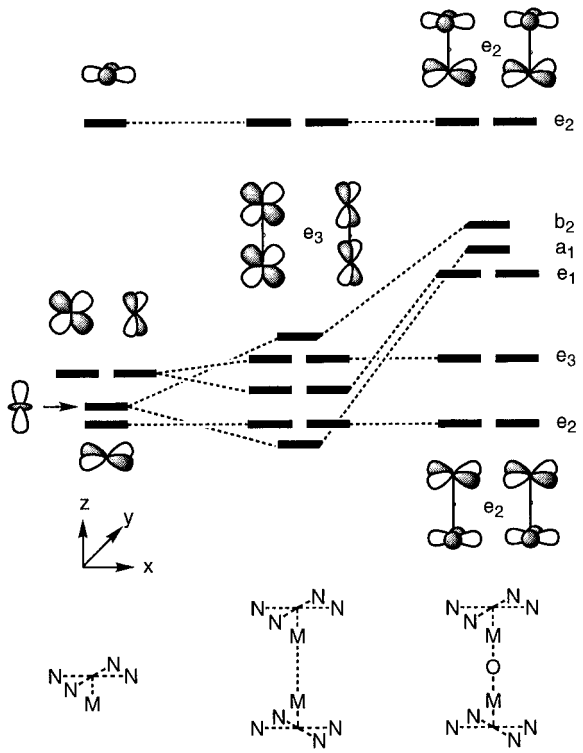

Figure 4. Building up of the orbitals of $[(NH_2^-)_4M\text{-}O\text{-}M(NH_2^-)_4]^{4-}$. From left to right: the orbitals of the pyramidal N_4M in which the M is 0.5 Å out of the N_4 plane; the orbitals of two N_4M units with an M−M separation of 3.526 Å; the orbitals of the composite oxo complex.

An examination of the electronic structure of μ-oxometalloporphyrin dimers provides an alternative rationale for the oxygen atom transfer chemistry of titanium porphyrins. The d-orbital energy level for $[Fe(TTP)]_2O$ shown in Figure 4 was derived by Tatsumi and Hoffmann[28] using extended Hückel calculations on $[(NH_2^-)_4Fe—O—Fe(NH_2^-)_4]^{4-}$ as a computational model. To a first approximation, this energy level diagram should apply to the $[(POR)M—O—M(POR)]^{0,+}$ (M = Cr, Ti) system. In the chromium case, when chromium(II) is the reductant, the neutral (POR)Cr−O−Cr(POR) dimer has six d-electrons. This leads to a $(e_2)^4(e_3)^2$ ground state which is electronically stable with respect to complete oxygen atom

(26) (a) Bottomley, L. A.; Kadish, K. M. *Inorg. Chem.* **1983**, *22*, 342−349. (b) Summerville, D. A.; Jones, R. D.; Hoffmann, B. M.; Basolo, F. *J. Am. Chem. Soc.* **1977**, *99*, 8195. (c) Basolo, F.; Jones, R. D.; Summerville, D. A. *Acta Chem. Scand., Ser. A* **1978**, *A32*, 771.

(27) (a) Liston, D. J.; Murray, K. S.; West, B. O. *J. Chem. Soc., Chem. Commun.* **1982**, 1109. (b) Liston, D. J.; West, B. O. *Inorg. Chem.* **1985**, *24*, 1568.

(28) (a) Tatsumi, K.; Hoffmann, R.; Whangbo, M.-H. *J. Chem. Soc., Chem. Commun.* **1980**, 509. (b) Tatsumi, K.; Hoffmann, R. *J. Am. Chem. Soc.* **1981**, *103*, 3328.

transfer. However, when chromium(III) is the reductant, the cationic d^5 μ-oxo species must have either a low-spin $(e_2)^4(e_3)^1$ or high-spin $(e_2)^2(e_3)^2(e_1)^1$ ground state. Either state is electronically degenerate and Jahn−Teller destabilized, leading to cleavage of the μ-oxo species. In similar manner, we can describe the titanium system. If titanium(II) is used as the reductant, the neutral μ-oxo species has a $(e_2)^2$ ground state which is electronically stable. When titanium(III) is used as the reductant, the cationic d^1 μ-oxo intermediate has a $(e_2)^1$ ground state and is electronically degenerate, leading to cleavage of the μ-oxo intermediate. Hence, the $O{=}Ti^{IV}/Cl{-}Ti^{III}$ reaction is electronically disposed toward complete oxygen atom transfer while the $O{=}Ti^{IV}/Ti^{II}$ system produces a stable μ-oxo product.

The $O{=}Ti/TiCl_2$ exchange, eq 6, is not predicted by a simple MO analysis. In this case, the putative $[Ti^{IV}{-}O{-}Ti^{IV}]^{6+}$ intermediate is d^0 and should be electronically stable. Furthermore, a neutral binuclear complex, Cl(TTP)Ti−O−Ti(TTP)Cl would appear to be a reasonable product. However, the formation of a strong Ti═O double bond again may be an important driving force. Mechanistically, the pseudooctahedrdal $(TTP)TiCl_2$ complex is unlikely to undergo an S_N2-type attack by the oxo complex. Prior dissociation of one of the chloride ligands is necessary to open a vacant coordination site. The positive $\Delta S^{\ddagger}$ for eq 6 suggests that Cl^- loss is the rate-determining step.

Concluding Remarks

A number of significant results have evolved from this study. Of particular interest is the observation that complete intermetal oxygen atom transfer is possible and facile for titanium porphyrins. Oxygen atom transfer in titanium porphyrin complexes can mediate both a one- and zero-electron process. The reversible processes reported here are the first such examples involving titanium porphyrins. It is clear that the oxo ligand is the preferred bridging species despite the presence of other good bridging ligands (e.g. chlorides and carboxylates). Finally, a simplified molecular orbital analysis suggests that the complete oxo transfer between (POR)Ti═O and (POR)-TiCl is promoted by electronic factors and the strong tendency for metal−oxygen double bond formation in a d° Ti(IV) complex.

Acknowledgment. Support for this work was provided by National Science Foundation Grant CHE-9057752 and the donors of the Petroleum Research Fund, administered by the American Chemical Foundation.

Supporting Information Available: Tables of crystallographic data, bond lengths and angles, anisotropic displacement factors, torsion angles, and hydrogen atom coordinates (17 pages). See any current masthead page for ordering information and Internet access instructions.

IC960863M